BK potassium channel modulation by leucine-rich repeat-containing proteins

Jiusheng Yan[1,2] and Richard W. Aldrich[1]

Section of Neurobiology, Center for Learning and Memory, University of Texas, Austin, TX 78712

Contributed by Richard W. Aldrich, April 2, 2012 (sent for review January 27, 2012)

Molecular diversity of ion channel structure and function underlies variability in electrical signaling in nerve, muscle, and nonexcitable cells. Regulation by variable auxiliary subunits is a major mechanism to generate tissue- or cell-specific diversity of ion channel function. Mammalian large-conductance, voltage- and calcium-activated potassium channels (BK, K_{Ca}1.1) are ubiquitously expressed with diverse functions in different tissues or cell types, consisting of the pore-forming, voltage- and Ca^{2+}-sensing α-subunits (BKα), either alone or together with the tissue-specific auxiliary β-subunits (β1–β4). We recently identified a leucine-rich repeat (LRR)-containing membrane protein, LRRC26, as a BK channel auxiliary subunit, which causes an unprecedented large negative shift (∼140 mV) in voltage dependence of channel activation. Here we report a group of LRRC26 paralogous proteins, LRRC52, LRRC55, and LRRC38 that potentially function as LRRC26-type auxiliary subunits of BK channels. LRRC52, LRRC55, and LRRC38 produce a marked shift in the BK channel's voltage dependence of activation in the hyperpolarizing direction by ∼100 mV, 50 mV, and 20 mV, respectively, in the absence of calcium. They along with LRRC26 show distinct expression in different human tissues: LRRC26 and LRRC38 mainly in secretory glands, LRRC52 in testis, and LRRC55 in brain. LRRC26 and its paralogs are structurally and functionally distinct from the β-subunits and we designate them as a γ family of the BK channel auxiliary proteins, which potentially regulate the channel's gating properties over a spectrum of different tissues or cell types.

accessory protein | patch clamp | signal peptide | cotranslational expression

Ion channels are membrane proteins responsible for electrical signaling in nerve, muscle, and nonexcitable cells. The diversity in electrical properties among different cell types or states is largely defined by expression and subunit composition of individual ion channel pore-forming principle subunits and often tissue- or cell type-specific regulatory subunits (1, 2). The large conductance, calcium- and voltage-activated potassium channel (BK, also termed as BK_{Ca}, Maxi-K, K_{Ca}1.1, or Slo1) is a unique member of the potassium channel family, which is dually activated by membrane depolarization and elevated intracellular free Ca^{2+} ($[Ca^{2+}]_i$), playing a powerful integrative role in the regulation of cellular excitability and calcium signaling (3). BK channels are critically involved in diverse physiological processes such as neuronal firing and neurotransmitter release (4), contractile tone of smooth muscles (5, 6), frequency tuning of auditory hair cells (7), and hormone secretion (8).

BK channels are homotetramers of the ubiquitously expressed, pore-forming, Ca^{2+}- and voltage-sensing α-subunits (BKα) either alone or in association with tissue-specific regulatory β-subunits. The four auxiliary β-subunits (β1–β4) are a family of 20- to 30-kDa two membrane-spanning homologous proteins with tissue-specific expression patterns, e.g., β1 is mainly found in smooth muscle and β4 in brain (9–11). We recently identified a leucine-rich repeat (LRR)-containing membrane protein, LRRC26, as a BK channel auxiliary subunit in lymph node carcinoma of the prostate (LNCaP) cells (12). LRRC26 causes an unprecedented large negative shift (∼ −140 mV) in voltage dependence of channel activation, allowing activation near resting voltages and $[Ca^{2+}]_i$ in excitable or nonexcitable cells (12). LRRC26 is structurally and functionally distinct from the four β-subunits and thus represents a different type of BK channel auxiliary subunit. Ion channel auxiliary subunits, such as the BK or Kv channel β-subunits, commonly exist in multiple paralogous forms with closely related modulatory functions. Here we have comparatively examined the modulatory effects and expression patterns of human LRRC26 and its paralogous proteins. Our results show that LRRC26 and its three paralogs, LRRC52, LRRC55, and LRRC38, have distinct tissue-specific expression patterns and graded capabilities in modulating the BK channel's voltage dependence of activation. We designate them as a γ family of the BK channel accessory subunits, which potentially regulate the channel's gating properties over a spectrum of different tissues or cell types.

Results

A LRR domain comprises repeating 20–29 residue leucine-rich sequence stretches, which contain a consensus sequence of LxxLxLxxN (where x can be any amino acid), and often two cysteine-rich sequences of variable length that cap the N- and C-terminal sides of the tandem LRR repeat units (13, 14). Among ∼400 LRR-containing proteins in the human protein database (UniProt), three LRRC26 paralogous proteins of unknown function, LRRC38, LRRC52, and LRRC55 (Fig. 1) have a protein size of ∼35 kDa and a predicted extracellular LRR domain structure and single transmembrane topology that are most closely related to LRRC26. Their amino acid sequence similarity of 30–40% is comparable to the sequence similarities among the BK channel β-subunits. As discussed later, we designate them as a group of BK channel γ-subunits. The amino acid sequences of LRRC26 and its three paralogous proteins are of high similarity in the structurally determinant residues of their LRR domains and become more divergent in the non-LRR regions (Fig. 1). Their N-terminal LRR domains comprise six LRR units in the middle and two cysteine-rich regions called LRRNT and LRRCT flanking on the N- and C-terminal sides, respectively.

LRRC26 and its paralogs all have a short N-terminal sequence containing a hydrophobic segment (HS) preceding the LRR domain (Fig. 1). These N-terminal regions are predicted to be signal peptides that are cleaved in the mature proteins and essential for extracellular translocation of the LRR domain, as demonstrated in some other LRR-containing proteins (15). To evaluate whether the N-terminal sequence can function as a cleavable signal peptide, a FLAG epitope tag was introduced at the N- or C-terminal side of the LRRC26's predicted N-signal peptide sequence. Immunoblot with an anti-FLAG antibody was performed to determine the retention or loss of the FLAG tag in the mature proteins (Fig. 2*A*). We observed that an N-terminally tagged

Author contributions: J.Y. and R.W.A. designed research; J.Y. performed research; J.Y. analyzed data; and J.Y. and R.W.A. wrote the paper.

The authors declare no conflict of interest.

[1]To whom correspondence may be addressed. E-mail: jshyan@mail.utexas.edu or raldrich@mail.utexas.edu.

[2]Present address: Department of Anesthesiology and Perioperative Medicine, University of Texas MD Anderson Cancer Center, Houston, TX 77030.

This article contains supporting information online at www.pnas.org/lookup/suppl/doi:10.1073/pnas.1205435109/-/DCSupplemental.

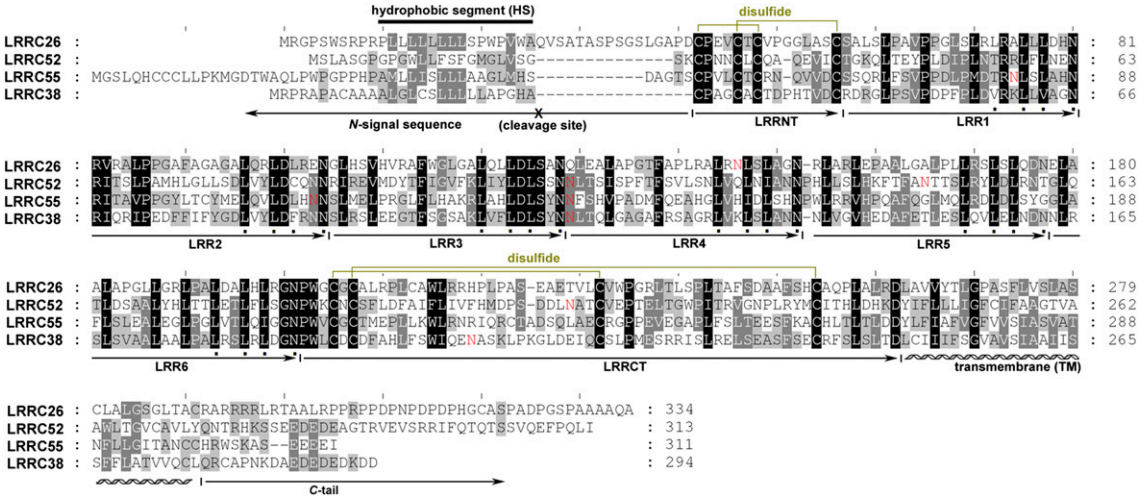

Fig. 1. Protein sequence alignment of human LRRC26 and its paralogs. Conserved residues are shaded at three levels (100, 80, and 50%). The hydrophobic segments and potential cleavage sites in the N-terminal signal peptide sequences are indicated. Potential N-glycosylation sites of Asn residues are shown in red. Cysteine pairs (four in total) for potential disulfide formation are indicated. Key residues of the consensus sequence (LxxLxLxxN) in each LRR unit are marked by a filled square at the bottom. The sequence similarities between LRRC26 and its paralogs are 38.2% (LRRC38), 33.4% (LRRC52), and 37.4% (LRRC55).

FLAG epitope was absent, whereas a C-terminally tagged FLAG behind the predicted cleavage site was retained in the mature LRRC26 protein when heterologously expressed in HEK-293 cells. Disruption of the signal peptide function by deletion of the hydrophobic segment (ΔHS) was able to block the cleavage and retain the N-terminally tagged FLAG in the expressed protein (Fig. 2*A*). Thus, the LRRC26's N-terminal sequence fully functions as an N-signal peptide that is cleaved in the mature protein.

Glycosylation is a commonly occurring posttranslational modification for extracellularly secreted proteins. LRRC26 and its paralogs' LRR domains all contain consensus N-glycosylation site (s), Asn–Xaa–Ser/Thr, where Xaa is not a proline. LRRC26 is predicted to be N-glycosylated at Asn147 in the middle of the LRR domain. We observed that the transiently expressed

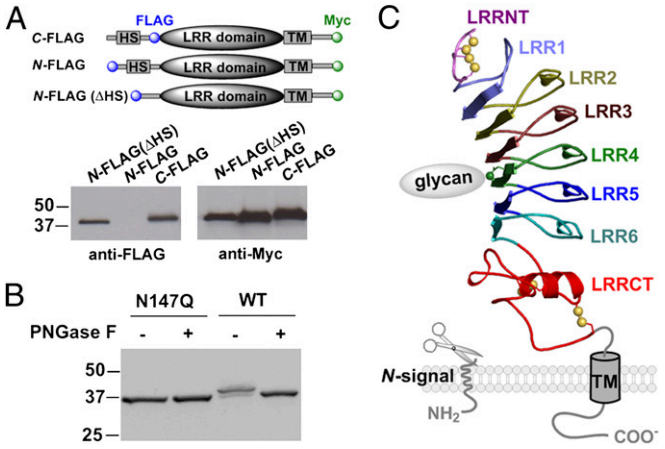

Fig. 2. Structural features of LRRC26. (*A*) Signal-peptide dependent cleavage of an N-terminally tagged FLAG epitope in mature protein as detected by immunoblots. (*B*) LRRC26 is glycosylated at an Asn147 site as detected by a loss of the PNGase treatment-induced mobility shift in N147Q mutant. (*C*) LRRC26's predicted membrane topology and LRR domain structure on the endoplasmic reticulum (ER) membrane. The LRR domain is N-glycosylated in the lumen of the ER and then exported to the extracellular side of plasma membrane. The sulfur atoms of the four cysteine pairs for potential disulfide formations are shown as bonded yellow balls. The nitrogen atom of Asn147 for N-glycosylation linkage is shown by a green sphere.

LRRC26 protein in HEK-293 cells can migrate as two molecular mass bands, a dominant upper band and a minor or barely visible lower band, in SDS/PAGE (Fig. 2*B*). Both the N147Q mutation and enzymatic removal of the N-linked glycan by PNGase F resulted in a disappearance of the upper glycosylated-mass band (Fig. 2*B*). This result is consistent with an extracellular location of the LRR domain in LRRC26.

An X-ray structure of LRRC26 or its paralogous proteins is not available. However, their LRR units are mostly canonical LRR units of 24 residues in length and their LRR N-terminal (LRRNT) and LRR C-terminal (LRRCT) regions' cysteine-rich sequences are similarly present in many other LRR-containing proteins. Thus, the LRR domain structures of LRRC26 and its paralogs can be modeled from known X-ray structures of other LRR-containing proteins, hagfish variable lymphocyte receptor B (16) for the LRRNT and LRR regions and mouse TLR4 (17) for the LRRCT region, on the basis of the amino acid sequence similarities in the corresponding regions (Fig. S1). Given the difference in the assignment of the start residue of the first LRR unit, the LRRC26's LRR region can be divided into five LRR units as annotated in the UniProt database and our previous report (12) or a structurally more appropriate separation into six similar LRR units (Figs. 1 and 2C). In the modeled structure of the LRRC26's LRR domain, the six stacked LRR units form a curved parallel β-sheet lining the concave face and small helices/turns flanking the convex circumference. The hydrophobic core of the LRR domain is tightly packed by the parallel inward-pointing leucine residues, shielded by the LRRCT and LRRNT caps on the N- and C-terminal ends. LRRC26 and its paralogs all contain four pairs of fully conserved cysteine residues in their LRRNT and LRRCT regions that potentially form four disulfide linkages in the favorable oxidizing extracellular environment (Figs. 1 and 2C).

We previously observed that the modulatory effect of LRRC26 on BK channels cannot be reliably or reproducibly measured in HEK-293 cells when the cDNA constructs of LRRC26 and BKα were simply mixed and cotransfected. This can be explained by disproportional uptake of the two cDNA constructs in a single cell during DNA transfection or insufficient plasma membrane expression of the LRRC26 protein in a heterologous expression system. We found that the LRRC26's N-signal sequence can be used as an internal cleavable signal peptide to allow efficient cotranslational protein synthesis and assembly of the stoichiometrically complexed BKα/LRRC26 channels when LRRC26 was

fused to the C terminus of BKα through its N terminus (12). Such an internal cleavage event was significantly blocked when the function of the signal peptide was disrupted by deletion of its hydrophobic segment (ΔHS) in the fusion construct of BKα and LRRC26. Consequently, the fused LRRC26 mutant (ΔHS) was unable to modulate BK channels presumably due to improper membrane topology (12). The signal peptide region, particularly its hydrophobic segment, in the precursor BKα–LRRC26 fusion protein is predicted to be cleaved from the mature BKα and LRRC26 proteins by signal peptidase and thus exerts minimal additional effect on the mature BK channel's gating properties. With this cotranslational expression method, we were able to obtain reproducible measurement of the electrophysiological properties of the LRRC26-complexed BK channels in HEK-293 cells (12). We found that the N-signal sequences of LRRC38, LRRC52, and LRRC55 can similarly function as fully cleavable internal signal peptides. Fusion constructs of BKα and LRRC26 paralogs expressed mature BKα and LRR proteins in similar molecular mass sizes as if they were individually expressed (Fig. S2). The BKα–LRRC55 fusion construct expressed a very low level of mature BKα protein, which generated a low level of BK channel current in some transfected cells but was not detectable by Western blot with anti-BKα antibody in our tested condition. Because the mature LRRC55 protein was still well expressed, this low level of BKα expression is likely due to degradation, resulting from C-terminal tagging of the LRRC55's long N-terminal fragment after signal peptidase cleavage. With these fusion/cotranslational expression constructs, we were able to measure reproducibly the modulatory effects of LRRC38, LRRC52, and LRRC55 on the BK channel's gating properties in HEK-293 cells by patch-clamp recording.

To evaluate whether they function as BK channel regulatory proteins, LRRC38, LRRC52, and LRRC55 were coexpressed with BKα in HEK-293 cells using the above cotranslational expression method. We previously reported that LRRC26 modified the BK channel's voltage dependence of activation by an ~ −140 mV shift of the $V_{1/2}$ (voltage of half maximal activation). We found that LRRC52, LRRC55, and LRRC38 are also able to modify the BK channel's voltage dependence of activation toward more negative voltages, but to different extents (Table S1). In the virtual absence of $[Ca^{2+}]_i$, LRRC52 and LRRC55 caused a large negative shift of the $V_{1/2}$ by −101 ± 4 mV and −51 ± 2 mV, respectively, and LRRC38 produced a smaller but reproducible shift of $V_{1/2}$ by −19 ± 1 mV (Fig. 3*A*). It is notable from a plot of $V_{1/2}$ vs. log $[Ca^{2+}]_i$ that the $V_{1/2}$ shifts caused by LRRC52 and LRRC55 in the presence of different concentrations of $[Ca^{2+}]_i$ (0.76–26 μM) are on average ~36 mV smaller than in the absence of $[Ca^{2+}]_i$ (Fig. 3 *A*–*C*), suggesting a modification in the apparent calcium sensitivity of BK channels by these two regulatory LRR proteins. According to the commonly used voltage and calcium-dependent allosteric gating model of BK channel activation, the apparent calcium sensitivity, which is defined as the slope in the $V_{1/2}$ vs. log $[Ca^{2+}]_i$ plot, can be affected by either a real change in microscopic calcium sensitivity (binding or allosteric coupling) or a modification in the voltage-related gating parameters (18, 19). Because the latter may result in a change in the shape of the normalized conductance vs. voltage (G–V) curve, a plot of the $Q_{app}V_{1/2}$ vs. log $[Ca^{2+}]_i$ was used to estimate whether the BK channel's microscopic calcium sensitivity is affected by these LRRC26 paralogs. Both $V_{1/2}$ and Q_{app} (apparent gating charge) are determined from a single Boltzmann function fit of the G–V curve (Table S1). A nonlinear relationship between the $Q_{app}V_{1/2}$ vs. log $[Ca^{2+}]_i$ was observed when all $[Ca^{2+}]_i$ conditions are included for plotting. As shown in Fig. 3*D*, LRRC26's three paralogs all cause slight changes in the relationship between $Q_{app}V_{1/2}$ and log $[Ca^{2+}]_i$, e.g., a slope change of ~20% by LRRC52 and LRRC38 and of ~40% by LRRC55 from 0.76 to 4.2 μM $[Ca^{2+}]_i$, suggesting some effects on the microscopic calcium sensitivity of BK channel activation. However, further detailed investigation in the context of the allosteric gating mechanism of BK channel activation by voltage and Ca^{2+} will be needed to separate the effects on Ca^{2+}- and voltage-activation pathways. Consistent with the different capabilities in inducing G–V shifts, LRRC26 and its paralogs modify the BK channel's K^+ current kinetics to different extents (Fig. S3). LRRC26 and its three paralogs all greatly increase the activation rates of BK channel currents. Additionally, LRRC26, LRRC52, and LRRC55 (at positive voltages) significantly decelerate channel deactivation, whereas a slight acceleration effect was also observed for LRRC38 and LRRC55 (at negative voltages).

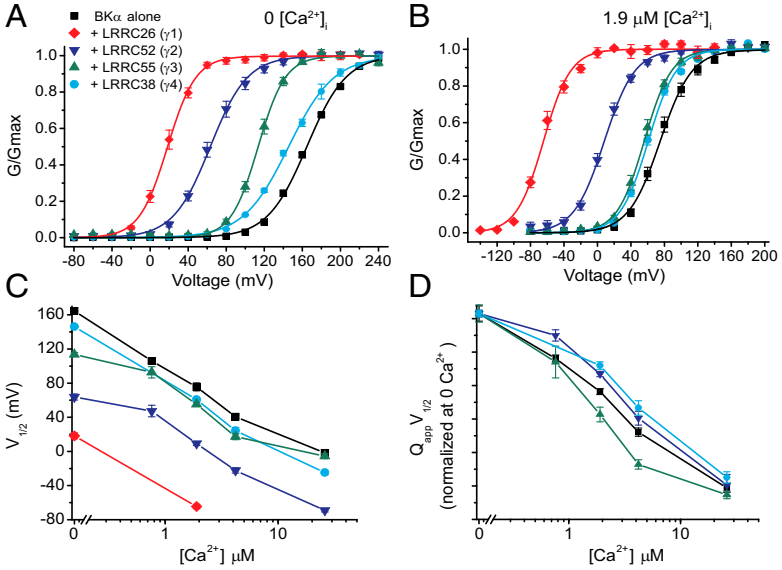

Fig. 3. Modulatory effects of LRRC26 and its paralogs on BK channels in HEK-293 cells. (*A* and *B*) Voltage dependence of the BK channel activation for the BKα alone or the BKα together with LRRC26, LRRC52, LRRC55, or LRRC38 in the virtual absence of $[Ca^{2+}]_i$ (*A*) or in the presence of 1.9 μM $[Ca^{2+}]_i$ (*B*). (*C*) Plot of $V_{1/2}$ vs. $[Ca^{2+}]_i$ (log scale after break). (*D*) Plot of $Q_{app}V_{1/2}$ vs. $[Ca^{2+}]_i$ normalized at 0 $[Ca^{2+}]_i$.

From the above results, we consider LRRC52, LRRC55, and LRRC38, together with previously reported LRRC26, a family of regulatory proteins of BK channels, which show graded capabilities in shifting the BK channel's voltage dependence of activation toward more negative voltages. Auxiliary subunits of ion channels, e.g., the BK channel β-subunits, commonly have tissue-specific expression patterns that fit different functional requirements of different cell types. To help estimate their physiological relevance in BK channel regulation, we quantitatively determined the expression profiles of LRRC26 and its three paralogs at the mRNA level in 20 different human tissues using the quantitative real-time PCR (qPCR) method. We observed that LRRC26 is highly expressed in normal human tissues of salivary gland, prostate, and trachea, and a moderate level of expression was found in thyroid gland, thymus, colon, aorta, and fetal brain (Fig. 4*B*). A low level of LRRC26 expression was also detected in lung, testis, adult brain, and cerebellum. LRRC52 is dominantly expressed in testis and skeletal muscle. A much lower level of LRRC52 expression was also detected in several other tissues including placenta, kidney, lung, and some glands. LRRC55 expression appears to be specific to the nervous system, which is most abundant in fetal brain and secondly in adult brain. LRRC38 is mainly expressed in skeletal muscle, adrenal gland and thymus, and a low level expression was also detected in brain and cerebellum.

Discussion

Among known accessory subunits of the voltage-gated ion channels, LRRC26 has a characteristic LRR domain structure and exerts a profound influence on voltage dependence of a voltage-gated ion channel. The LRR domain in many proteins is known to provide a structural framework for protein–protein interactions, typically through the concave β-sheet side (13). LRRC26 and its three paralogs, LRRC52, LRRC55, and LRRC38 thus represent a unique type of ion channel auxiliary protein family. These proteins cause marked and graded modulation in the BK channels' voltage dependence of activation and exhibit tissue-specific expression patterns. They are distinct from the four BK channel β-subunits in both structures and modulatory effects. For convenience, we designate them as a family of BK channel γ-subunits, e.g., LRRC26 as γ1, LRRC52 as γ2, LRRC55 as γ3, and LRRC38 as γ4, in the order of magnitude of their modulatory effects on BK channel gating.

LRRC26 and its three paralogs belong to a previously grouped "Elron" subfamily of the "extracelluar LRR"-containing proteins, which also contain two additional proteins, LRTM1 and LRTM2 (20). The six LRR-containing proteins in the Elron subfamily were considered to be "LRR_only" (absence of other classified protein domain) proteins of low stringency (20), which are mainly present in mammals and defined as paralogs in the Ensembl database. However, LRTM1 and LRTM2 contain an additional extracellular LRR-unrelated segment of ∼50 residues located between the LRRCT and the transmembrane (TM) regions, which is fully absent in LRRC26, LRRC38, LRRC52, and LRRC55 (Fig. S1). Our functional analyses indicated that LRTM1 and LRTM2, unlike the other four members, have no significant modulatory effect on the BK channel's gating properties when they were coexpressed with BKα in HEK-293 cells (Fig. S4). LRTM1 and LRTM2 are hereby tentatively not considered as functional paralogs of LRRC26 in BK channel modulation.

The γ-subunits are similarly related to each other in overall protein sequence. However, they display very different capabilities in shifting the BK channel's $V_{1/2}$ in the absence of $[Ca^{2+}]_i$ by ∼ −140 mV (γ1 or LRRC26), −100 mV (γ2 or LRRC52), −50 mV (γ3 or LRRC55), and −20 mV (γ4 or LRRC38). Our

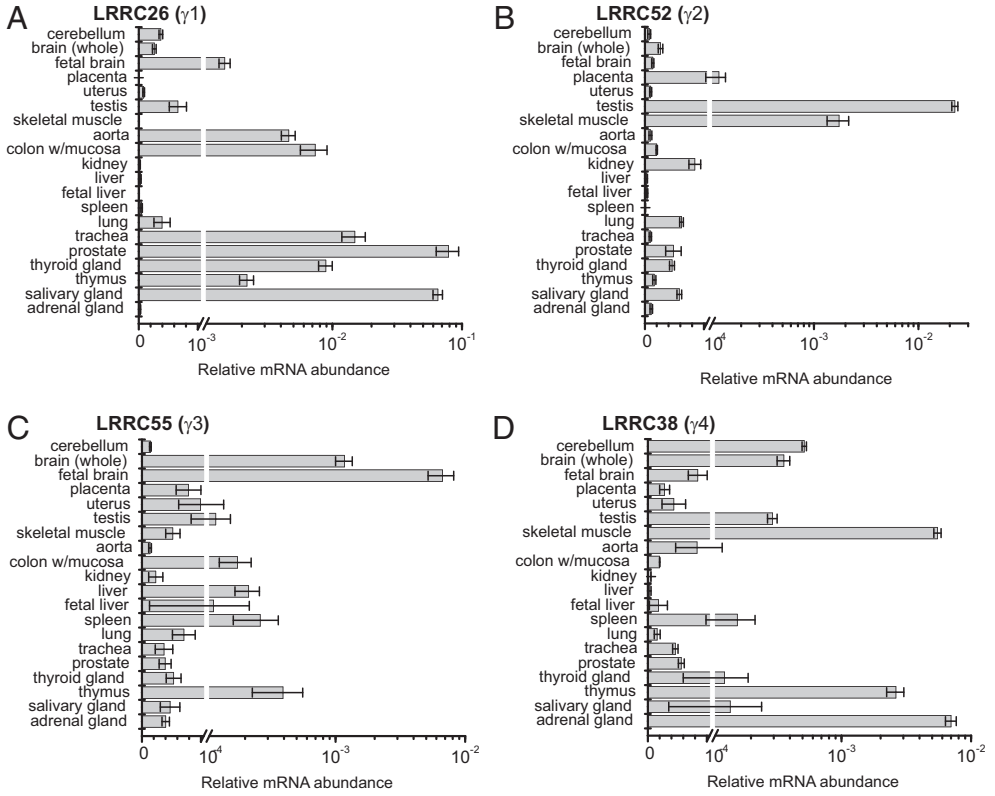

Fig. 4. Relative expression levels of LRRC26 and its paralogs in different human tissues. The relative expression level of each individual LRR protein was detected by quantitative TaqMan real-time PCR. RPLPO (large ribosomal protein) was used as a reference gene for internal control. The relative mRNA abundance is plotted in log scale after break.

previous mutagenesis studies indicated that most parts of the γ1 protein are necessary for its modulatory function, suggesting that γ1 might work as a whole in BK channel modulation (12). Thus, it is difficult to predict from the protein sequences how γ1 and its three paralogs are different in BK channel modulation. The observed smaller shifts in voltage dependence of BK channel activation caused by γ2 (LRRC52) and γ4 (LRRC38) than γ1 (LRRC26) might be partly explained by their lower expression level relative to the BKα protein in the cotranslational/fusion expression condition, which can be caused by degradation and is expected to result in variability in the bound γ-subunits per BK channel complex and consequently decreased apparent gating charges or slopes of the observed G–V curves. However, γ2 is notably different from γ1 in its effects on the rates of BK channel deactivation at very negative voltages, e.g., −120 mV (Fig. S3). Additionally, a similar extent of BK channel modulation was observed when γ-subunits were coexpressed with BKα separately (non-cotranslationally) in HEK-293 cells (Fig. S5). It remains to be determined whether the difference in glycosylation status among these LRR proteins contributes to their difference in BK channel modulation.

The γ-subunits are distinct from the four BK channel β-subunits in their modulatory effects. The β-subunits drastically decrease both the activation and deactivation rates of the BK channel currents and only slightly modify the apparent voltage dependence in the absence of $[Ca^{2+}]_i$, although β1 can exceptionally cause an ∼ −30- to −50-mV shift of voltage dependence at high $[Ca^{2+}]_i$ (≥10 μM) conditions through an enhanced calcium sensitivity (10, 11, 21, 22). The γ-subunits rather markedly shift the BK channel's voltage dependence of channel activation in the negative direction in the absence of $[Ca^{2+}]_i$. From a plot of the $Q_{app}V_{1/2}$ vs. log $[Ca^{2+}]_i$, γ-subunits, particularly γ3 (LRRC55), might exert some effects on the BK channel's calcium sensitivity (Fig. 3). It is notable that they all contain a short stretch of acidic residues, $_{282}$EEDEDE$_{287}$ (γ2 or LRRC52), $_{307}$EEEE$_{310}$ (γ3 or LRRC55), and $_{286}$EDEDED$_{291}$ (γ4 or LRRC38), in their intracellular C terminus (Fig. 1), resembling the "Ca^{2+}-sensing" acidic clusters found in the BKα subunit's RCK domain and in the C terminus of bestrophin-1 (23). These acidic residue clusters might potentially affect the Ca^{2+} sensitivity of channel activation through a direct Ca^{2+} association or by interactions with the BKα's Ca^{2+}-docking sites.

We previously observed that the β1 subunit when overexpressed can functionally compete with γ1 (LRRC26), suggesting some commonly shared mechanism in physical association or modulatory action between these two distinct types of BK channel regulatory proteins (12). Like the β-subunits, the TM domain in γ1 is essential for its modulatory function and physical association with the BKα (12). It remains unclear whether the β- and γ-subunits' extraceullar or transmembrane domains are sterically exclusive on the BK channel complex.

Similar to tissue-specific expression of the four BK channel β-subunits (10), the four γ-subunits show tissue-specific expression patterns in the 20 different human normal tissues tested. Consistent with its abundant expression in human salivary gland as detected in this study, γ1 (LRRC26) in mouse parotid acinar cells explains the hyperpolarized activation of endogenous BK channels (24) and also interestingly the loss of the channels' sensitivity to the potent activator mallotoxin (25). In secretory glands or epithelial cells, γ1 activates BK channels and thus facilitates the channel's function in fluid and electrolyte secretion. γ1 may additionally account for the low-voltage–activated BK channels observed in breast cancer cells (26), inner ear hair cells (27), and arterial smooth muscle cells (28–31). LRRC26 was recently reported to suppress tumor growth and metastasis (32), agreeing with its high expression in the early stage prostate cancer LNCaP cells and diminished expression in the very late stage prostate cancer PC-3 cells (12, 33). γ2 (LRRC52) predominantly expresses in testis and skeletal muscle. Similar to the observed modulatory effect of the BK channel β-subunits on the closely related Slo3 channels, a recent study indicates that γ2 (LRRC52) is also a candidate regulatory subunit of the Slo3 channels in sperm cells (34). Expression of BKα is highest in the premeiotic germ cells but lowest in the postmeiotic germ cells (35). γ2 (LRRC52) in germ cells may modulate both BK and Slo3 channels in a cell-stage–dependent manner. Among all tested human tissues, γ3 (LRRC55) was most strongly expressed in the brain. According to the γ3 gene expression map obtained with EGFP BAC transgenic mice, GFP protein under the control of endogenous γ3 transcriptional regulatory elements was well expressed in many different regions or tissues of fetal and adult mouse brains, including the mitral cell layer of olfactory bulb, medial habenular nuclei of thalamus, ventral tegmental area (VTA), substantia nigra, and cortex (http://www.gensat.org). The specific expression of γ3 in the nervous system may provide a mechanism of BK channel activation that is more responsive to membrane depolarization preceding $[Ca^{2+}]_i$ elevation. The greatly diminished activating effect of γ3 upon $[Ca^{2+}]_i$ increase may prevent BK channels from being overactive during an action potential in excitable cells.

Materials and Methods

Expression of BKα and LRRC26 or Its Paralogs in HEK-293 Cells. Recombinant cDNA constructs of human BKα and LRRC26 and its paralogs were used for heterologous expression in HEK-293 cells. Cloned or synthetic cDNA sequences of human LRRC26, LRRC38, LRRC52, and LRRC55 were subcloned into the mammalian expression vector of pCDNA6, with FLAG and V5 tags attached at their C termini. Fusion cDNA constructs, which encode precursor fusion proteins of human BKα and C-terminally tagged LRR proteins, were generated with pCDNA6 vector and used to facilitate cotranslational assembly of the BKα/LRR protein complexes after endogenous cleavage by peptidases at the linker (signal peptide) region in the mature proteins. HEK-293 cells were obtained from ATCC and transfected with the designed plasmid(s) using Lipofectamine 2000 (Invitrogen), and used within 16–72 h for electrophysiological assays or at ∼48 h for biochemical assays.

Structural Modeling. A structural model of the LRRC26's LRR domain was built by homology modeling with SWISS MODEL and SWISS-pdb viewer (36). The crystal structure of hagfish variable lymphocyte receptor B (16) [Protein Data Bank (PDB) ID code 2O6S; amino acids 24–187] was used as a template for the homology modeling of the LRRNT and the six LRR units of LRRC26. The structure of the LRRC26's LRRCT region was modeled with the crystal structure of mouse TLR4 (17) (PDB ID code 2Z64; amino acids 583–625).

Electrophysiology. The BK channel's gating properties including voltage and Ca^{2+} dependence, and K^+ current kinetics were determined by patch-clamp recording in excised inside-out patches of HEK-293 cells with symmetric solutions of 136 mM KMeSO3, 4 mM KCl, and 20 mM Hepes (pH 7.20) supplemented with 2 mM $MgCl_2$ for external solution and a certain amount of $CaCl_2$ buffered by 5 mM HEDTA or nitrilotriacetic acid for internal solution. The free Ca^{2+} concentration in the internal solution ($[Ca^{2+}]_i$) was measured with a Ca^{2+}-sensitive electrode (Orion Research). The steady-state activation was expressed as G/G_{max} calculated from the relative amplitude of the tail currents (deactivation at −120 mV). The voltage of half-maximal activation ($V_{1/2}$) and the equivalent gating charge (z) were obtained by fitting the relations of G/G_{max} vs. voltage with single Boltzmann function $G/G_{max} = 1/(1 + e^{-zF(V-V1/2)/RT})$. SEM was used to plot error bars for variation in experimental values.

Quantitative Expression Analyses. Total RNA samples of 20 different human tissues (Clontech, human total RNA master panel) were used for expression analyses of LRRC26 and its three paralogs by quantitative real-time PCR. The fist-strand cDNA was synthesized from a template of total RNA using reverse transcriptase with primer of oligo(dT). TaqMan real-time PCR was performed to quantitate the amount of synthesized cDNA of a target gene. LRRC26 and its paralogs are all encoded by two exons. To ensure specificity, the probes were designed to encompass the connecting sites of the two exons. The following forward and reverse primers and probes were used: LRRC26, 5′-CGCGTCAGAGGCCGAG-3′, 5′-TGGCTAAAGGCGGCGTC-3′, and 5′-6FAM-ACGCCTGACGCTCAGCCCCC-TAM-3′; LRRC52, 5′-TCCTGGACTTCGCCATCTTC-3′, 5′-TCAGCTCTGTGGGCTCCAC-3′, and 5′-6FAM-CATATGGACCCCTCAGATGATCTAAATGCC-TAM-3′; LRRC55, 5′-TGGCAATCCCTGGGTGTG-3′, 5′-AGCCAGC-

PHYSIOLOGY

TGAGAATCTGCTGTAC-3′, and 5′-6FAM-CTGCTGAAGTGGCTGCGAAACCG-TAM-3′; LRRC38, 5′-TGGATCCAGGAGAACGCATC-3′, 5′-TATCCTCCTGCTCTCCATGGG-3′, and 5′-6FAM-AAGGCCTTGATGAAATCCAGTGCTCCC-TAM-3′. The efficiency of target amplification with the designed primers and probes were validated with templates of serially diluted plasmid DNA. Human RPLPO (large ribosomal protein) endogenous control (primer and FAM/MGB probe; Invitrogen) was used as an internal control for comparision among different RNA samples.

ACKNOWLEDGMENTS. We thank Chris Lingle and Chengtao Yang for discussion. Work was supported in part by National Institutes of Health Grant NS075118 (to J.Y.).

1. Schulte U, Müller CS, Fakler B (2011) Ion channels and their molecular environments—glimpses and insights from functional proteomics. *Semin Cell Dev Biol* 22:132–144.
2. Pongs O, Schwarz JR (2010) Ancillary subunits associated with voltage-dependent K^+ channels. *Physiol Rev* 90:755–796.
3. Berkefeld H, Fakler B, Schulte U (2010) Ca^{2+}-activated K^+ channels: From protein complexes to function. *Physiol Rev* 90:1437–1459.
4. Gribkoff VK, Starrett JE, Jr., Dworetzky SI (2001) Maxi-K potassium channels: Form, function, and modulation of a class of endogenous regulators of intracellular calcium. *Neuroscientist* 7:166–177.
5. Brayden JE, Nelson MT (1992) Regulation of arterial tone by activation of calcium-dependent potassium channels. *Science* 256:532–535.
6. Brenner R, et al. (2000) Vasoregulation by the beta1 subunit of the calcium-activated potassium channel. *Nature* 407:870–876.
7. Ramanathan K, Michael TH, Jiang GJ, Hiel H, Fuchs PA (1999) A molecular mechanism for electrical tuning of cochlear hair cells. *Science* 283:215–217.
8. Petersen OH, Maruyama Y (1984) Calcium-activated potassium channels and their role in secretion. *Nature* 307:693–696.
9. Uebele VN, et al. (2000) Cloning and functional expression of two families of beta-subunits of the large conductance calcium-activated K^+ channel. *J Biol Chem* 275: 23211–23218.
10. Brenner R, Jegla TJ, Wickenden A, Liu Y, Aldrich RW (2000) Cloning and functional characterization of novel large conductance calcium-activated potassium channel beta subunits, hKCNMB3 and hKCNMB4. *J Biol Chem* 275:6453–6461.
11. Behrens R, et al. (2000) hKCNMB3 and hKCNMB4, cloning and characterization of two members of the large-conductance calcium-activated potassium channel beta subunit family. *FEBS Lett* 474:99–106.
12. Yan J, Aldrich RW (2010) LRRC26 auxiliary protein allows BK channel activation at resting voltage without calcium. *Nature* 466:513–516.
13. Kobe B, Kajava AV (2001) The leucine-rich repeat as a protein recognition motif. *Curr Opin Struct Biol* 11:725–732.
14. Ng AC, et al. (2011) Human leucine-rich repeat proteins: A genome-wide bioinformatic categorization and functional analysis in innate immunity. *Proc Natl Acad Sci USA* 108(Suppl 1):4631–4638.
15. Chan DV, et al. (2011) Signal peptide cleavage is essential for surface expression of a regulatory T cell surface protein, leucine rich repeat containing 32 (LRRC32). *BMC Biochem* 12:27.
16. Kim HM, et al. (2007) Structural diversity of the hagfish variable lymphocyte receptors. *J Biol Chem* 282:6726–6732.
17. Kim HM, et al. (2007) Crystal structure of the TLR4-MD-2 complex with bound endotoxin antagonist Eritoran. *Cell* 130:906–917.
18. Cui J, Aldrich RW (2000) Allosteric linkage between voltage and $Ca^{(2+)}$-dependent activation of BK-type mslo1 $K^{(+)}$ channels. *Biochemistry* 39:15612–15619.
19. Horrigan FT, Aldrich RW (2002) Coupling between voltage sensor activation, Ca^{2+} binding and channel opening in large conductance (BK) potassium channels. *J Gen Physiol* 120:267–305.
20. Dolan J, et al. (2007) The extracellular leucine-rich repeat superfamily; a comparative survey and analysis of evolutionary relationships and expression patterns. *BMC Genomics* 8:320.
21. Cox DH, Aldrich RW (2000) Role of the beta1 subunit in large-conductance $Ca^{(2+)}$-activated $K^{(+)}$ channel gating energetics. Mechanisms of enhanced $Ca^{(2+)}$ sensitivity. *J Gen Physiol* 116:411–432.
22. Solaro CR, Lingle CJ (1992) Trypsin-sensitive, rapid inactivation of a calcium-activated potassium channel. *Science* 257:1694–1698.
23. Xiao Q, Prussia A, Yu K, Cui YY, Hartzell HC (2008) Regulation of bestrophin Cl channels by calcium: Role of the C terminus. *J Gen Physiol* 132:681–692.
24. Romanenko VG, Thompson J, Begenisich T (2010) Ca^{2+}-activated K channels in parotid acinar cells: The functional basis for the hyperpolarized activation of BK channels. *Channels (Austin)* 4:278–288.
25. Almassy J, Begenisich T (2012) The LRRC26 protein selectively alters the efficacy of BK channel activators. *Mol Pharmacol* 81:21–30.
26. Gessner G, et al. (2005) BK_{Ca} channels activating at resting potential without calcium in LNCaP prostate cancer cells. *J Membr Biol* 208:229–240.
27. Thurm H, Fakler B, Oliver D (2005) Ca^{2+}-independent activation of BK_{Ca} channels at negative potentials in mammalian inner hair cells. *J Physiol* 569:137–151.
28. Sansom SC, Stockand JD (1994) Differential Ca^{2+} sensitivities of $BK_{(Ca)}$ isochannels in bovine mesenteric vascular smooth muscle. *Am J Physiol* 266:C1182–C1189.
29. Benham CD, Bolton TB, Lang RJ, Takewaki T (1986) Calcium-activated potassium channels in single smooth muscle cells of rabbit jejunum and guinea-pig mesenteric artery. *J Physiol* 371:45–67.
30. Toro L, Vaca L, Stefani E (1991) Calcium-activated potassium channels from coronary smooth muscle reconstituted in lipid bilayers. *Am J Physiol* 260:H1779–H1789.
31. Jackson WF, Blair KL (1998) Characterization and function of $Ca^{(2+)}$-activated K^+ channels in arteriolar muscle cells. *Am J Physiol* 274:H27–H34.
32. Liu XF, et al. (2011) CAPC negatively regulates NF-kappaB activation and suppresses tumor growth and metastasis. *Oncogene* 31:1673–1682.
33. Egland KA, et al. (2006) High expression of a cytokeratin-associated protein in many cancers. *Proc Natl Acad Sci USA* 103:5929–5934.
34. Yang C, Zeng XH, Zhou Y, Xia XM, Lingle CJ (2011) LRRC52 (leucine-rich-repeat-containing protein 52), a testis-specific auxiliary subunit of the alkalization-activated Slo3 channel. *Proc Natl Acad Sci USA* 108:19419–19424.
35. Gong XD, Li JC, Leung GP, Cheung KH, Wong PY (2002) A $BK_{(Ca)}$ to $K_{(v)}$ switch during spermatogenesis in the rat seminiferous tubules. *Biol Reprod* 67:46–54.
36. Arnold K, Bordoli L, Kopp J, Schwede T (2006) The SWISS-MODEL workspace: A web-based environment for protein structure homology modelling. *Bioinformatics* 22: 195–201.